

# Common and unusual diseases involving the iliopsoas muscle compartment: spectrum of cross-sectional imaging findings

Massimo Tonolini, Alessandro Campari, Roberto Bianco

Department of Radiology, “Luigi Sacco” University Hospital, Via G.B. Grassi 74, 20157 Milan, Italy

## Abstract

Although relatively uncommon, many different infectious, hemorrhagic and neoplastic disease processes may involve the iliac and psoas muscles and are increasingly diagnosed especially in referral hospitals. Furthermore, the iliopsoas compartment may become injured during trauma, percutaneous instrumentation, laparoscopic or open surgical procedures. State-of-the-art cross-sectional imaging including volumetric multidetector CT and multiplanar MRI acquisitions allows prompt detection, comprehensive visualization and confident characterization of most iliopsoas lesions, and the possibility to guide percutaneous biopsy and drainage. The pertinent regional anatomy is reviewed in correlation with disease pathways and imaging modalities. Neoplastic lesions, purulent and mycobacterial iliopsoas infections are discussed with examples. Imaging plays the key role in the differentiation of primary versus secondary abscesses due to intestinal, urinary and musculoskeletal infections, that determines medical therapy and surgical need. The iliopsoas compartment may become involved through direct extension by retroperitoneal, skeletal and pelvic tumors, and should be carefully scrutinized when reviewing oncologic imaging studies since it represents one of the preferred sites of skeletal muscle metastatization. Iliopsoas hemorrhages due to trauma, aortic aneurysms and anticoagulation are reviewed, with a special focus on determining whether the bleeding comes from aneurysmal rupture or from coagulopathy, a critical differentiation to decide about medical or surgical treatment. Postoperative complications involving the iliopsoas compartment are discussed with examples, including retroperitoneal bleeding, infections, urinary leaks and collections following various surgical or instrumentation procedures. Emphasis is placed on

choosing the correct imaging modality and technique, particularly to detect active bleeding or urine leakage, and to reduce artifacts related to presence of metallic implants.

**Key words:** Iliopsoas muscle—Iliopsoas abscess—Musculoskeletal tuberculosis—Skeletal muscle metastasis—Haemorrhage—Urinoma—Iatrogenic—Postoperative complications—Computed tomography (CT)—Magnetic resonance imaging (MRI)

## Anatomy and imaging

The iliopsoas compartment, delimited by its namesake fascia, is an extraperitoneal space including the major and minor psoas together with the iliac muscle bellies, that act as flexors of the thigh and trunk and lateral flexors of the spine [1].

The major (greater) psoas muscle originates proximally from the lateral aspect and transverse processes of T12 and lumbar vertebrae, and extends inferiorly into the pelvis to merge with the iliac muscle, arising from the internal aspect of the iliac wing. Together they cross inferiorly beneath the inguinal ligament to form a common distal tendon that inserts on the lesser femoral trochanter. The inconstant minor (lesser) psoas muscle arises from the T12-L1 vertebral bodies and inserts on the ileopectineal eminence [1, 2].

Asymmetry in muscle size between the left and right side may be present in healthy individuals, particularly in association with spinal scoliosis. Muscular hypertrophy (in athletes) or fatty atrophy (in elderly, debilitated, or immobile patients) is sometimes observed.

Involvement of the iliopsoas muscles in many different disease processes is explained mainly by its close anatomic proximity to the lumbar spine and bony pelvis muscles posteriorly, and to the retroperitoneal organs

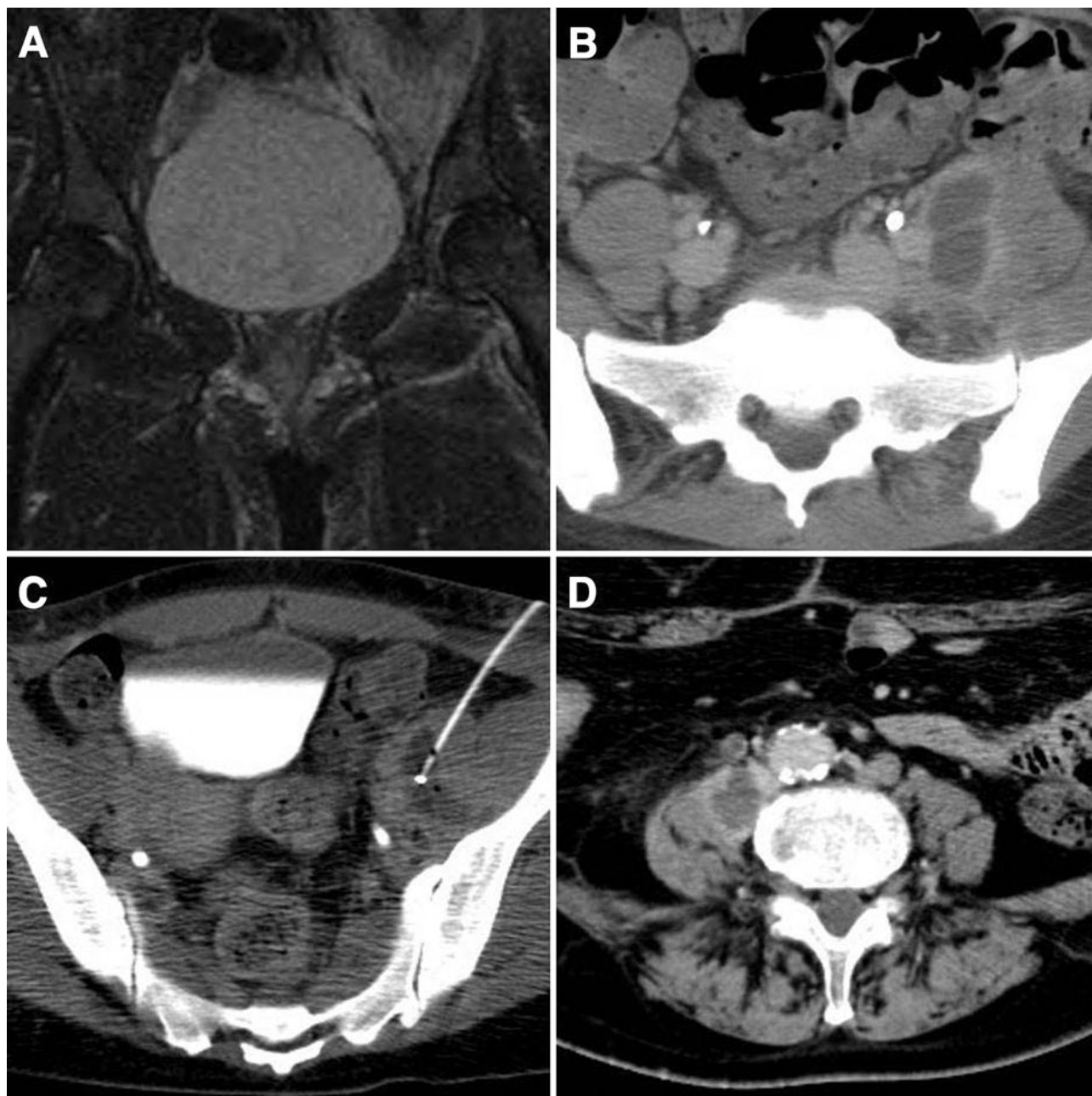


**Fig. 1.** Primary psoas abscess in a 33-year-old HIV-positive female patient. Coronal STIR image (**A**) from focused sacro-iliac MRI examination requested for lumbosacral pain shows diffuse hyperintensity involving the left iliopectus muscle. Axial postcontrast CT image (**B**) shows biloculated peripherally enhancing collection in the thick-

ened psoas, causing medial dislocation of the ipsilateral ureter. CT-guided drainage was performed on the iliopectus portion (**C**). Axial contrast-enhanced CT image (**D**) shows primary right iliopectus abscess in another, 51-year-old female patient hospitalized with *St. aureus* sepsis from unknown source

(including the kidneys and aorta) and some bowel segments anteriorly. Furthermore, the iliopectus compartment constitutes a communication from the thorax to the pelvis and proximal femur, that can function as a pathway for distant disease spread [3].

The deep, retroperitoneal location explains the often indolent presentation of many pathologic

processes involving the iliopectus muscles. Before the advent of current cross-sectional imaging modalities, diagnosis of pathologic iliopectus conditions was usually late.

Ultrasound is usually insufficient to diagnose or exclude iliopectus abnormalities because the retroperitoneum may be difficult to visualize confidently, and its

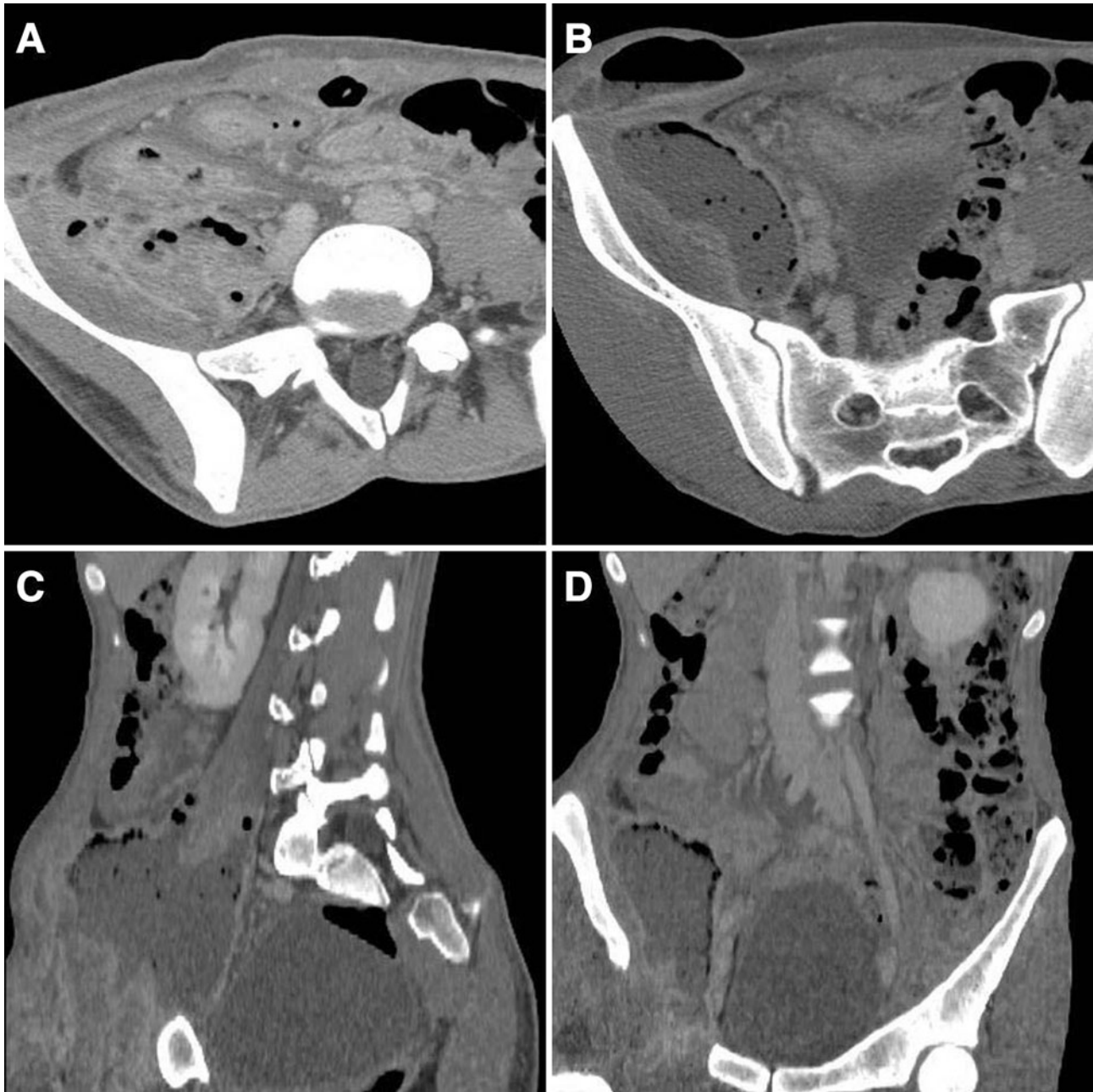


**Fig. 2.** 21-year-old male patient affected by active Crohn's Disease. Axial CT image (**A**) depicts fistulization of the involved ileal loop into the right psoas muscle, markedly inhomogeneous with serpiginous contrast enhancement

and gas bubbles. Caudal axial image (**B**) plus sagittal (**C**) and coronal (**D**) reformations depict the large iliopsoas abscess in its entirety, with extension to the cutaneous plane

sensitivity is estimated to approach 60% [4]. Contrast-enhanced CT is the mainstay imaging modality to assess retroperitoneal diseases, particularly in the acute setting, and is currently performed with multidetector volumetric acquisitions: multiplanar reformations along the coronal and sagittal planes are best suited to assess the iliopsoas muscle bellies according to their principal axis, thus

providing better depiction of disease spread [5]. Although less widely available, MRI has two important advantages over CT, including ideal visualization of spine abnormalities on sagittal-oriented images, and better assessment of bone marrow and soft tissues involvement by disease thanks to fat-suppression techniques.

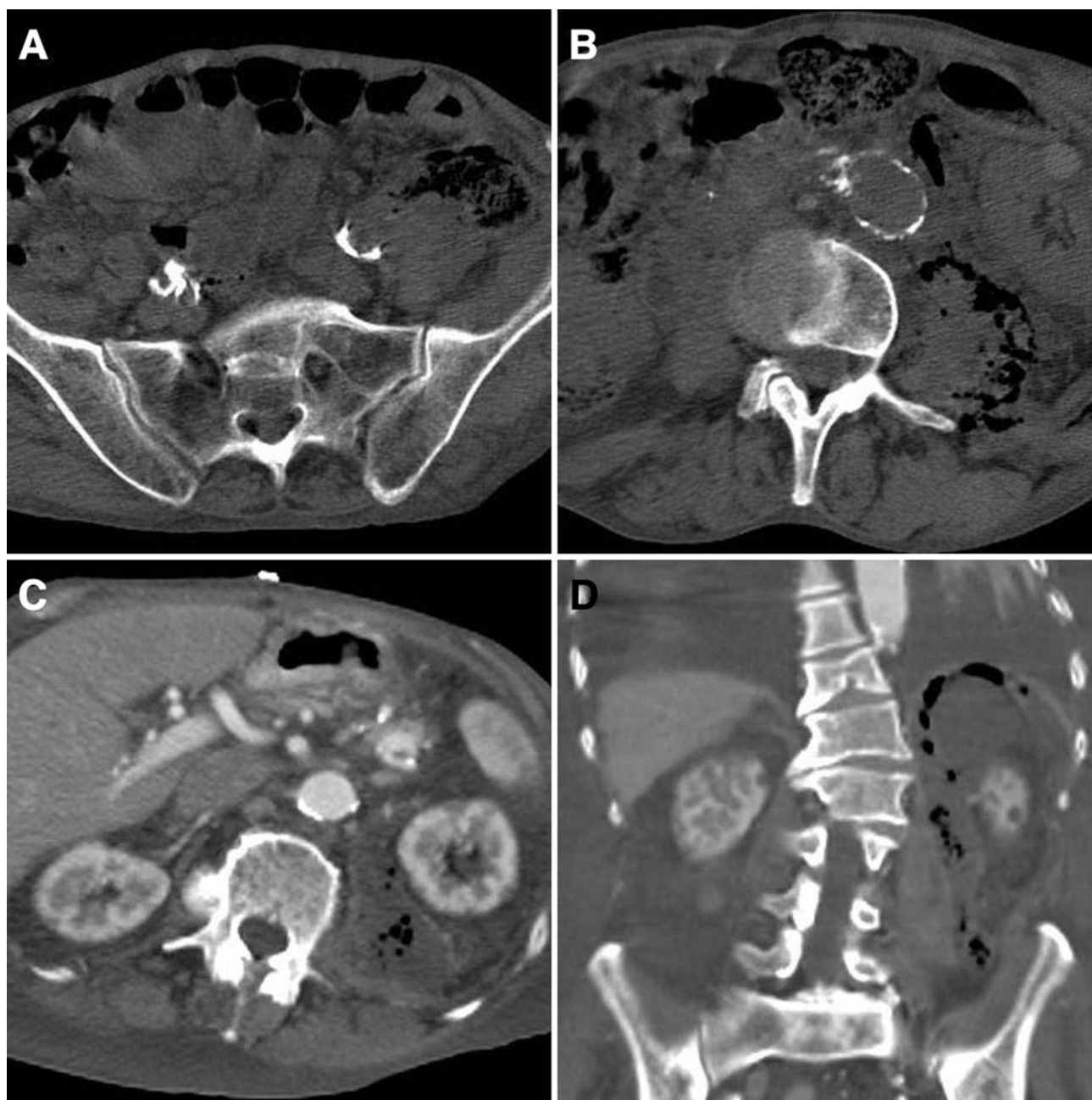


**Fig. 3.** Emergency CT in an elderly 87-year-old male with acute abdomen. Unenhanced scans show wall thickening of the proximal sigmoid colon with some upstream dilatation consistent with stricturing primary cancer (**A**), enlarged left

psoas muscle with diffuse air bubbles (**B**) due to retroperitoneal neoplastic perforation. Enhanced axial (**C**) and coronal-reformatted (**D**) images confirm diffuse psoas infection by enteric organisms

## Infections and neoplastic lesions

### *Purulent infections*

An iliopsoas abscess is an increasingly diagnosed and potentially life-threatening condition, currently not exceptional in busy, major hospitals [2, 6]. Its clinical manifestation is variable, with the classic triad of

symptoms (including fever, flank pain, limping or hip flexion) reported in less than half of patients; an indolent presentation with vague abdominal complaints, back pain, malaise, and weight loss is not uncommon particularly in patients with impaired cognitive status or immune responses, resulting in a delayed diagnosis [4, 6, 7]. Laboratory inflammatory abnormalities including raised



**Fig. 4.** Elderly 93-year-old female patient with right pyelonephritis and pyonephrosis with calcific calyceal stones and associated ipsilateral psoas abscess (**A**, **B**). Resolution of

psoas collection was obtained after percutaneous drainage and subsequent nephrostomy

white-cell count, ESR, and C-reactive proteins are usually present; hemocultures may reveal the causative organism, thus providing causal therapy [4].

Pyogenic infections are classified as primary and secondary abscesses.

Primary iliopsoas abscesses are diagnosed when no obvious local cause can be identified, and attributed to hematogenous spread of a distant, sometimes occult infectious process; *Staphylococcus aureus* is by far the most common pathogen [3, 4, 6–9]. Currently, most series report a very low incidence (less than 20% of all cases) of primary abscesses, usually diagnosed in association with Acquired Immunodeficiency Syndrome (AIDS), intravenous drug abuse, immunosuppression, or diabetes mellitus (Fig. 1) [1, 4, 6–9].

More commonly, psoas abscesses are secondary and originate through direct infectious spread from adjacent organs including the small and large bowel, the kidneys and urinary tract, the spine or the aorta. Gastrointestinal causes include fistulizing Crohn's disease as the most frequent one (up to 60% of cases) (Fig. 2), diverticulitis, complicated acute appendicitis, perforated colorectal cancer (Fig. 3), and typhlitis [4, 6, 7, 10–13]. Infectious spread through the perirenal space and fasciae in patients with acute pyelonephritis and/or infected hydronephrosis may give rise to psoas abscess lesions (Fig. 4) [7]. Additionally, secondary iliopsoas abscesses may result from extension of musculoskeletal infections such as pyogenic spondylo-diskitis (in nearly 20% of cases)

(Fig. 5) or septic sacro-iliitis (Fig. 6) [7, 14, 15]. Even more uncommon causes of psoas abscesses include aortic prosthesis or aortic aneurysm infections [16].

In secondary psoas abscesses, pathogens are usually multiple and include mostly enteric pathogens, *E.coli*, *Bacteroides*, and *Streptococcus*; conversely *Staphylococcus aureus* is the usual organism found in more than half of cases resulting from spinal osteomyelitis [4, 6, 15].

Currently, CT represents the mainstay imaging modality, as it provides quick, early, and accurate diagnosis of iliopsoas infection even in acutely ill patients, and usually allows to define the abscess as secondary by displaying an underlying primary disease [5, 7].

Iliopsoas abscesses manifest at CT with variable enlargement of the involved muscle belly compared to the contralateral, caused by a hypoattenuating, sometimes multiloculated lesion showing peripheral “rim” enhancement after intravenous contrast (Figs. 1, 2, 3, 4, 5, 6) [1–4, 7, 9].

Ancillary findings consistent with infection include indistinct margins, obliteration of the surrounding fat planes, sometimes air-fluid levels and bone destruction; although uncommon, the presence of gas bubbles is considered specific (Figs. 2,3) [1, 7]. Differentiation of an abscess from hematoma (characteristically hyperdense on unenhanced CT scans) and tumor may prove challenging, so the radiologist needs support from pertinent clinical information.

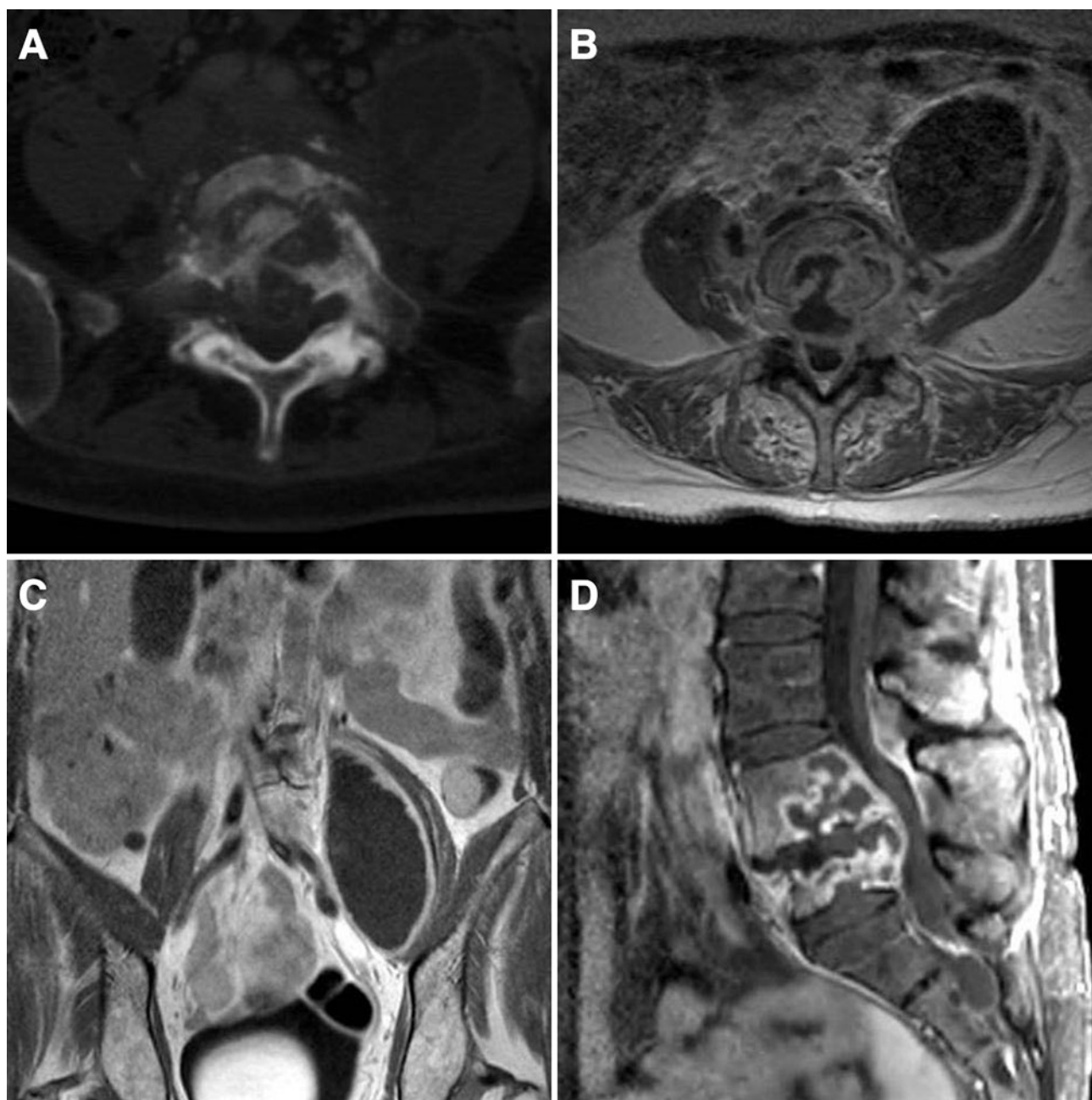


**Fig. 5.** Pelvic CT image viewed at bone window (**A**) in a 40-year-old HIV-positive male shows destruction of vertebral endplates and tumefaction of the left psoas muscle. Corresponding post-contrast axial T1-weighted MR image (**B**) depicts enhancing border of enlarged and liquefied intervertebral

disk, communicating with a large left psoas abscess, entirely visualized on a coronal enhanced T1-weighted image (**C**). Sagittal post-contrast fat-suppressed T1 sequence reveals L4-L5 spondylo-diskitis (due to *St. Aureus*) as the primary infection underlying psoas abscess

MRI is particularly suited when musculoskeletal infection is suspected, due to exquisite detection of bone marrow infectious involvement; muscle abscesses appear as fluid-like cavities with low T1-weighted, high T2 signal intensity, and intense peripheral enhancement (Figs. 5, 6) [2, 3, 14, 15].

Early and correct diagnosis and treatment are important since untreated infection may progress to sepsis and local complications such as perforation: iliopsoas abscesses have a nonnegligible mortality, reaching 20% in patients with secondary lesions [6].

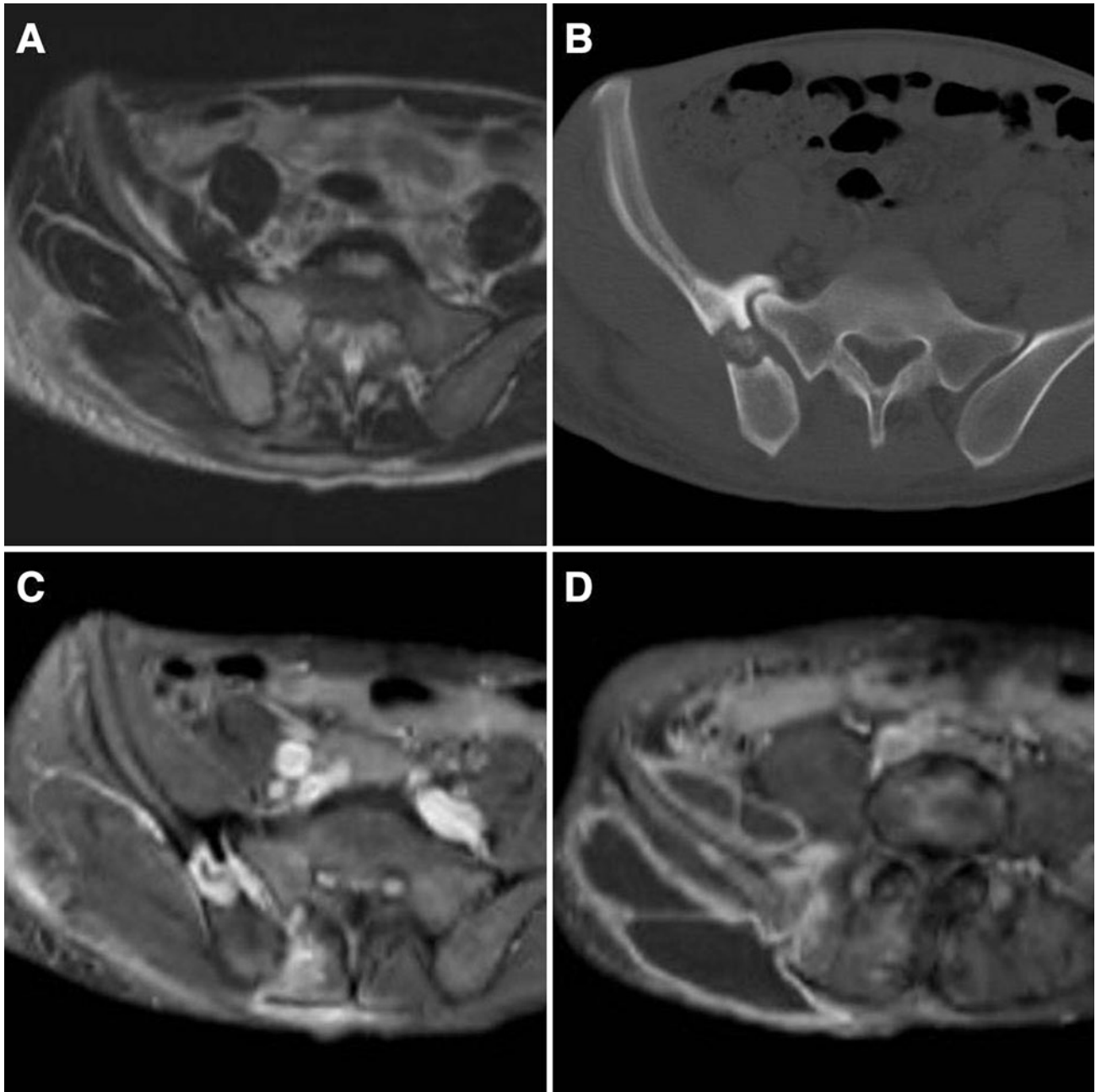


**Fig. 6.** 30-year-old female patient with history of trauma several weeks earlier, complaining of pain in the right iliac fossa and gluteal region. Axial T2-weighted image (**A**) shows abnormally increased signal intensity involving the right sacroiliac joint space and both facing bony surfaces; corresponding bone-window CT image (**B**) shows sclerosis

and lytic changes with a sequestrum in the right iliac wing. Post-contrast axial T1-weighted image shows intense enhancement consistent with acute infection in the joint space and in the iliac lytic focus (**C**). Abscess collections extend to the ipsilateral gluteal and iliac muscles (**D**)

Imaging differentiation between primary and secondary abscesses is paramount since in patients with primary lesions and spinal infections anti-Staphylococcal antibiotics should be started immediately before culture results, since nearly 9 out of 10 lesions result from *St. aureus* infections. Conversely, when a secondary

infection (with the exception of spondylodiskitis) is diagnosed, broad-spectrum antibiotics should be started [4].

Treatment of iliopsoas abscesses is based on appropriate antibiotics, coupled with drainage [4]. Small abscesses are usually treated effectively with antibiotics

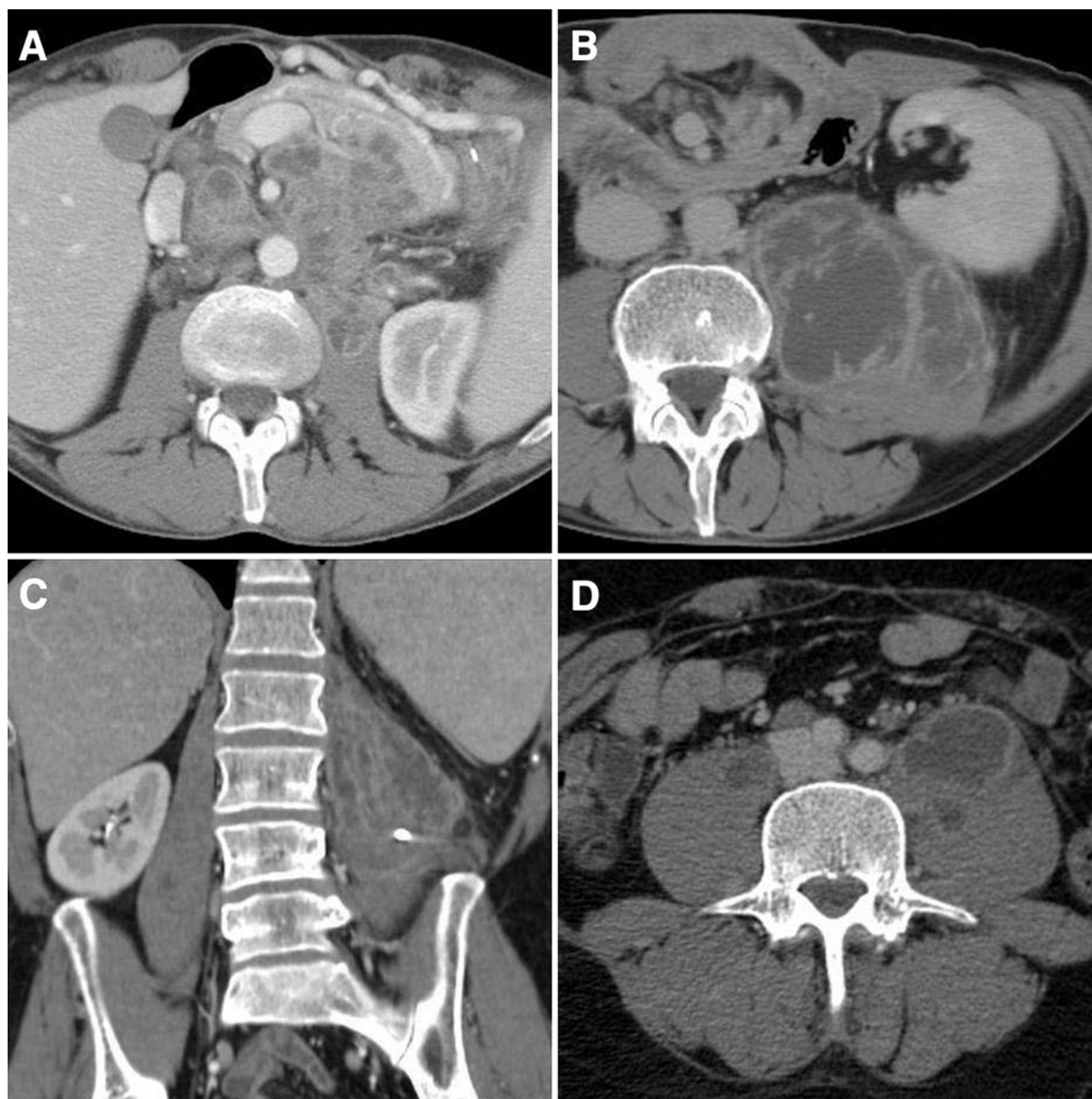


**Fig. 7.** 31-year-old HIV-positive male with opportunistic atypical mycobacteriosis (*M. Avium Intracellulare*) involving the mesenteric and retroperitoneal lymph nodes with extension to the left psoas muscle (**A**). Progressively enlarging

mycobacterial psoas abscess (**B**) was treated by drainage (**C**). Bilateral psoas abscesses due to *M. tuberculosis* (**D**) in another patient with AIDS

alone. Ultrasound or CT-guided aspiration is useful to confirm the diagnosis, obtain microbiology specimen, and position percutaneous drainage which is usually therapeutic (Figs. 1, 4, 7) [2]. The Trocar technique is adopted for large unilocular collections, whereas the modified Seldinger is preferred with smaller abscesses or when percutaneous approach is felt to be technically

challenging. Usually, 6 to 8 French catheters are used, whereas viscous fluids need larger (10–12 Fr) drainage.

With the exception of associated intestinal lesions requiring excision, treatment of iliopsoas abscesses is rarely surgical, and an open surgery should be reserved for complicated or recurrent lesions [17].



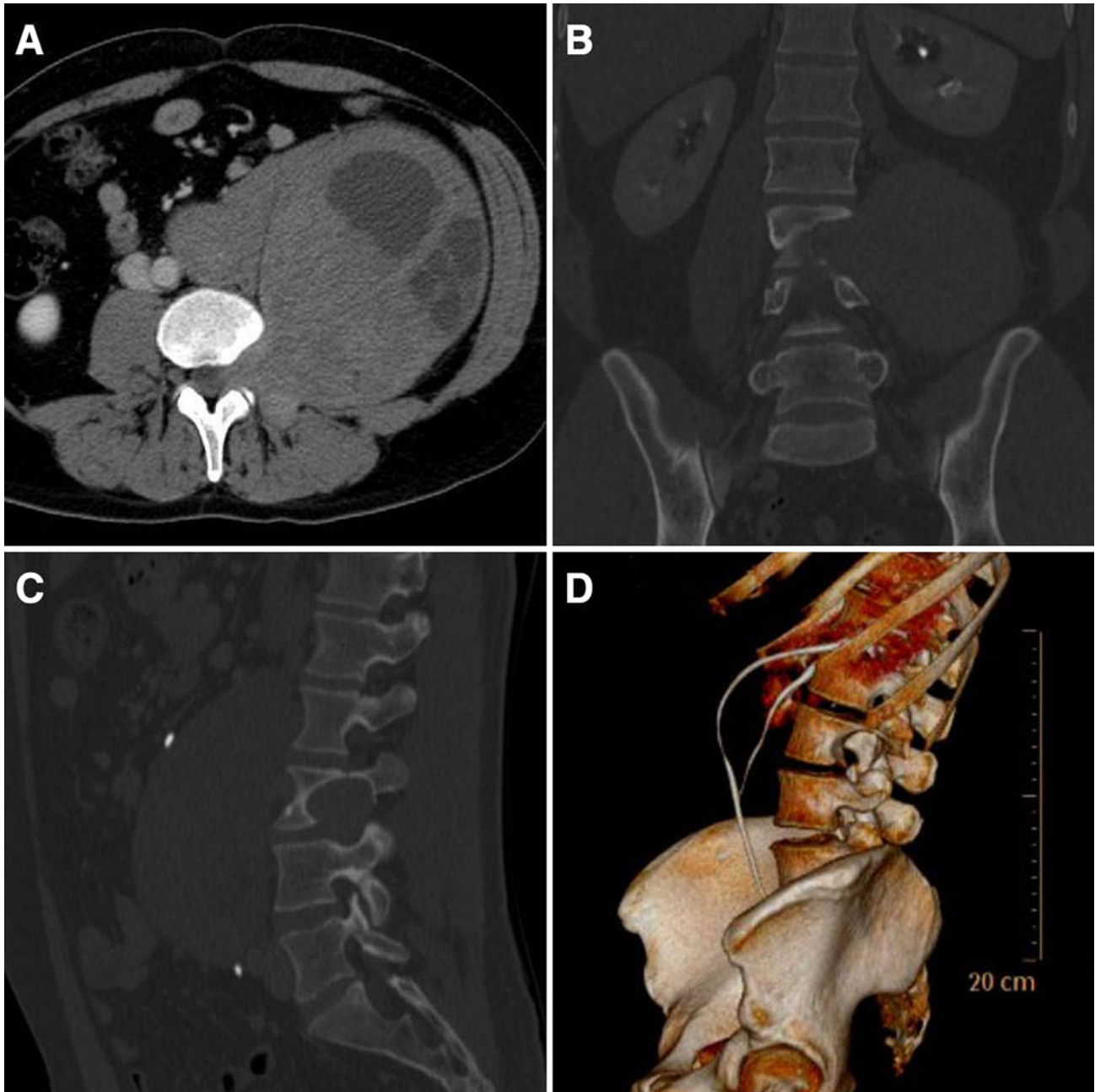


**Fig. 8.** Schwannoma in a 31-year-old male. After ultrasound detection (not shown) of a large space-occupying lesion in the left abdomen, axial contrast-enhanced CT image (**A**) confirms huge expansile, partly necrotic lesion originating from the L3-L4 neural foramen with associated para-aortic lymphadenopathy, that encompasses the ipsilateral psoas muscle. Coronal (**B**) and sagittal (**C**) reformations viewed at bone window, 3D volume-rendered image (**D**) document widening and remodeling of the neural foramen, plus ventral ureteral displacement

nopathy, that encompasses the ipsilateral psoas muscle. Coronal (**B**) and sagittal (**C**) reformations viewed at bone window, 3D volume-rendered image (**D**) document widening and remodeling of the neural foramen, plus ventral ureteral displacement

### *Mycobacterial infections*

In the past, spinal tuberculosis (Pott's disease) was the leading cause of paraspinous abscesses. After the eradication of *M. tuberculosis* in the developed world, during

the 1980s pyogenic bacteria became the predominant etiology of iliopsoas infections.

More recently, a resurgence of specific infections has been observed, especially in immigrants, HIV-infected or



◀ **Fig. 9.** Intractable lumbosacral pain in a 64-year-old male. Axial T1- (**A**) and T2-weighted (**B**) MR images depict a large paravertebral solid mass incorporating the left psoas muscle and ventrally displacing the retroperitoneal large vessels. Image from CT-guided biopsy (**C**) shows lysis of the vertebral body and transverse process. Pathology-diagnosed extramedullary plasmocytoma

otherwise immunosuppressed patients, usually with a subtle clinical presentation [1, 6, 18, 19]. Furthermore, in the same patients up to 5%–30% of diagnosed musculoskeletal mycobacterial infections are caused by atypical *M. species*, although with similar imaging appearances (Fig. 7) [20, 21].

Mycobacterial psoas involvement is often but not invariably associated with spinal tuberculosis, since infection may extend from the vertebral bodies through the periosteum to the paraspinal muscles, giving rise to complex multilocular ossifluent abscesses [22, 23]. Subligamentous spread to three or more vertebral levels with or without skip lesions, the relative preservation of the intervertebral disk, large and/or paravertebral soft-tissue abscesses with well-defined and sometimes calcified wall are reported as suggestive features to differentiate specific vs. pyogenic spinal infections [22, 24].

Alternatively, psoas abscesses can be associated with centrally nonenhancing, caseating retroperitoneal, inguinal, and mesenteric lymphadenopathies in the setting of abdominal mycobacteriosis without demonstrable spine infection (Fig. 7) [19, 25].

### *Neoplastic lesions*

Although uncommon, the iliopsoas compartment may be involved by neoplastic disease through direct extension of adjacent retroperitoneal neurogenic (Fig. 8), skeletal (Fig. 9), or abdomino-pelvic (mainly colonic and urogenital) (Fig. 10) tumors. Cross-sectional imaging is usually helpful in identifying the origin of these masses. Conversely, primary psoas muscle tumors such as liposarcoma and fibrosarcoma are exceedingly rare [1, 3, 26].

Although skeletal muscles make up nearly half of body mass, hematogenous metastatization to the muscle is very uncommon due to the combined effect of contraction during movement, variability of blood flow, unfavorable pH, and effect of protease inhibitors [26, 27]. Along with the paravertebral and gluteal muscles, the iliopsoas ranks among the preferred sites of skeletal muscle metastases, usually diagnosed in patients with disseminated neoplastic disease from gastrointestinal, urological, and genital primary tumors, sometimes from

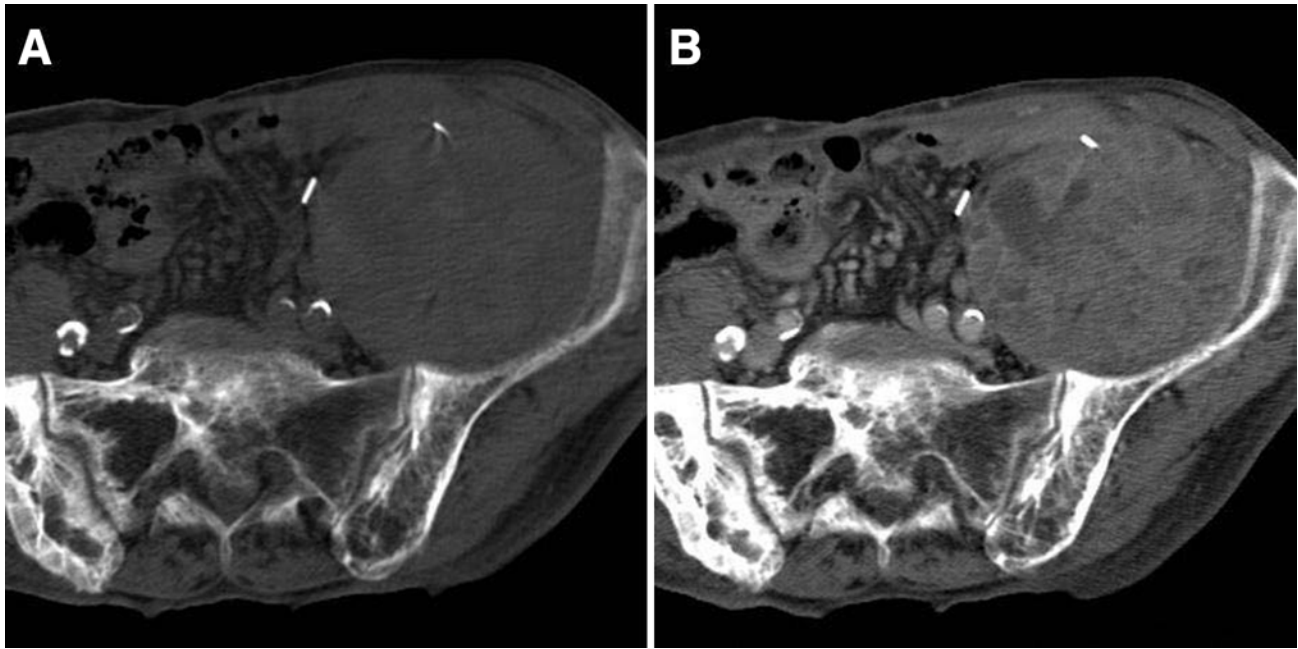


**Fig. 10.** 77-year-old male patient with previous resection of sigmoid neoplasm. Follow-up CT (unenhanced bone-window image in **A**, post-contrast soft tissue in **B**) shows involvement of the left iliac muscle by a large expansile lesion bordered by

surgical clips with an inhomogeneous, partly necrotic appearance, and absent osteolysis. Biopsy confirmed colon cancer local recurrence

melanoma and lung cancer (Fig. 11) [26, 27]. Alternatively, the iliopsoas belly may be invaded by skeletal metastases (Fig. 11).

Therefore, careful scrutinizing of the above-mentioned muscles is strongly suggested when reviewing follow-up studies in oncologic patients. Psoas metastases usually show nonspecific imaging appearances with muscle enlargement, round or oval shape, low CT attenuation values, hypointense T1- and hyperintense T2-weighted MR signal, variable contrast enhancement; calcifications may be observed in some histological types (Fig. 11) [3, 26]. Differentiation of neoplastic from infectious lesions is not always possible with confidence, since in nearly one-third of cases skeletal metastases show an abscess-like appearance, whereas bone destruction and lymphadenopathy may be associated with both. Percutaneous biopsy may be requested when confirmation of metastatic nature may alter the patient's therapeutic approach (Fig. 9) [27].

### **Hemorrhages, urinary leaks, iatrogenic, and postoperative lesions**

Currently, an increasing incidence of iliopsoas abnormalities results from the widespread use of anticoagulation medications and the proliferation of urologic, vascular, and orthopedic instrumentation and surgical

procedures, with increased likelihood of retroperitoneal bleeding, infectious and urinary complications [2].

### *Hemorrhages*

Hemorrhage involving the iliopsoas muscle is a relatively uncommon occurrence, and may be observed after trauma, with ruptured aortic aneurysm or vascularized tumors such as renal angiomyolipoma, and in association with bleeding diathesis or anticoagulation [1–3].

Currently, thanks to its availability, speed and diagnostic potential, multidetector CT is the mainstay imaging modality to assess both trauma and acute abdomen in the emergency setting [1, 28].

Hematomas tend to involve the psoas or iliac muscles diffusely, causing enlargement of the muscular belly. The CT appearance of muscle hematomas depends on the entity and speed of the bleeding. Fresh blood has high attenuation values (up to 80 HU) and appears hyperdense compared to the soft tissue and normal muscular bellies. Over time, decreasing attenuation leads to a characteristic mixed-density appearance with fluid–fluid levels (the so-called “hematocrit effect”) corresponding to stratification of different hematic components. Chronic hematomas tend to become hypodense and are not easily differentiated from abscess collections or tumors, so correlation with appropriate clinical history is necessary [1–3].

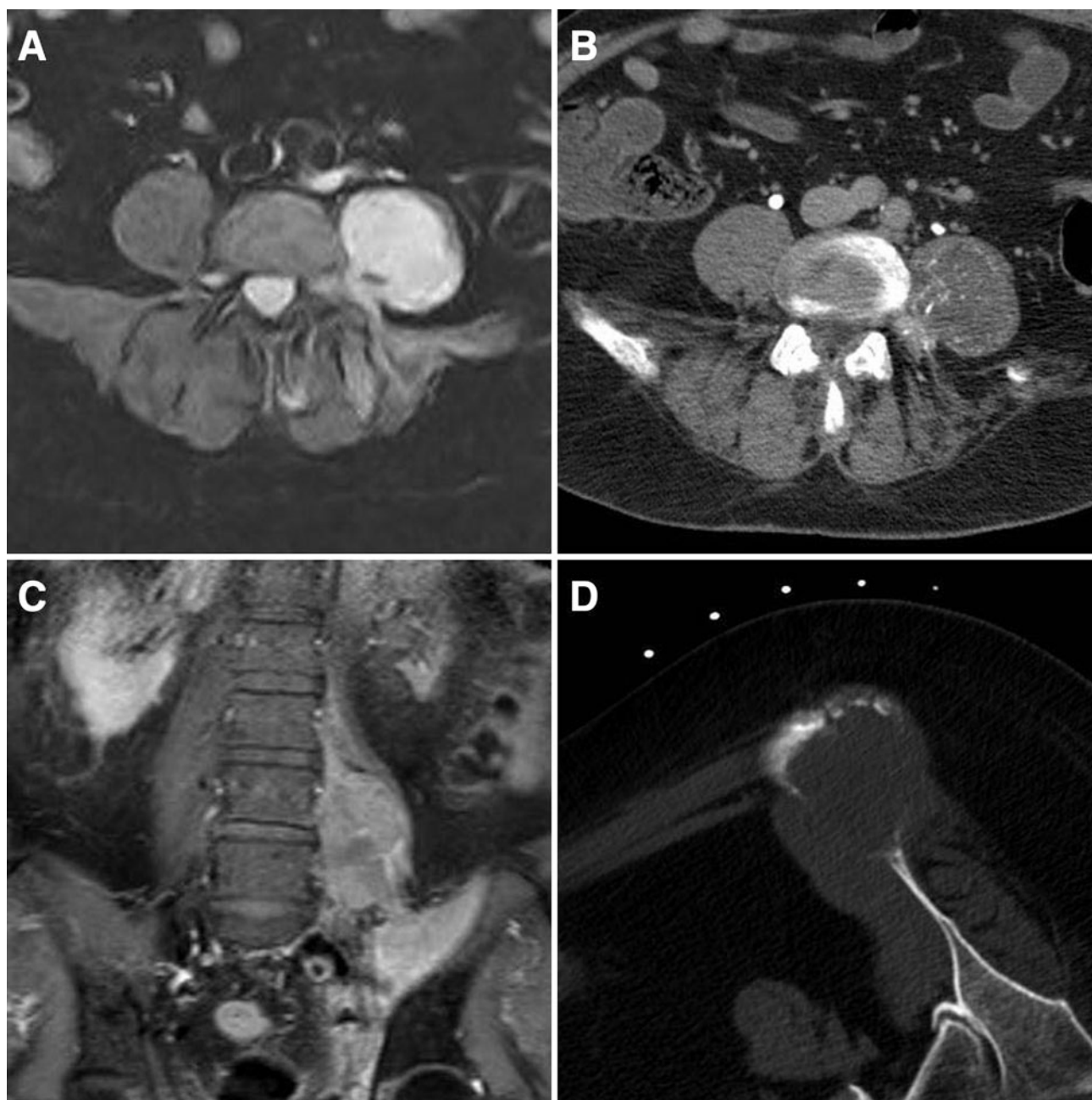


**Fig. 11.** 64-year-old male with history of cystectomy for bladder carcinoma. Follow-up MRI shows diffuse signal hyperintensity on STIR images (**A**) involving the left psoas muscle, with corresponding CT hypodensity with speckled calcifications (**B**). Post gadolinium fat-suppressed coronal T1 image (**C**) documents homogeneous enhancement of the

metastatic lesion, plus involvement of the ipsilateral iliac muscle. In a 71-year-old female previously treated for breast cancer, pre-biopsy unenhanced CT scan (**D**) shows aggressive skeletal metastasis invading the contiguous iliac muscle, incidentally discovered during follow-up

Contrast injection is useful to assess hemorrhagic lesions, since arterial- and portal phase acquisitions during enhanced CT may reveal contrast extravasation consistent with active bleeding, usually best visualized using high-flow injection [1, 29].

Thanks to the well-known signal intensity variation over time, MRI may be useful to judge about the age an hematoma, usually visualized with T1 hyperintensity in subacute bleeding, with hypointense signal particularly at the periphery in chronic ones [1, 3].

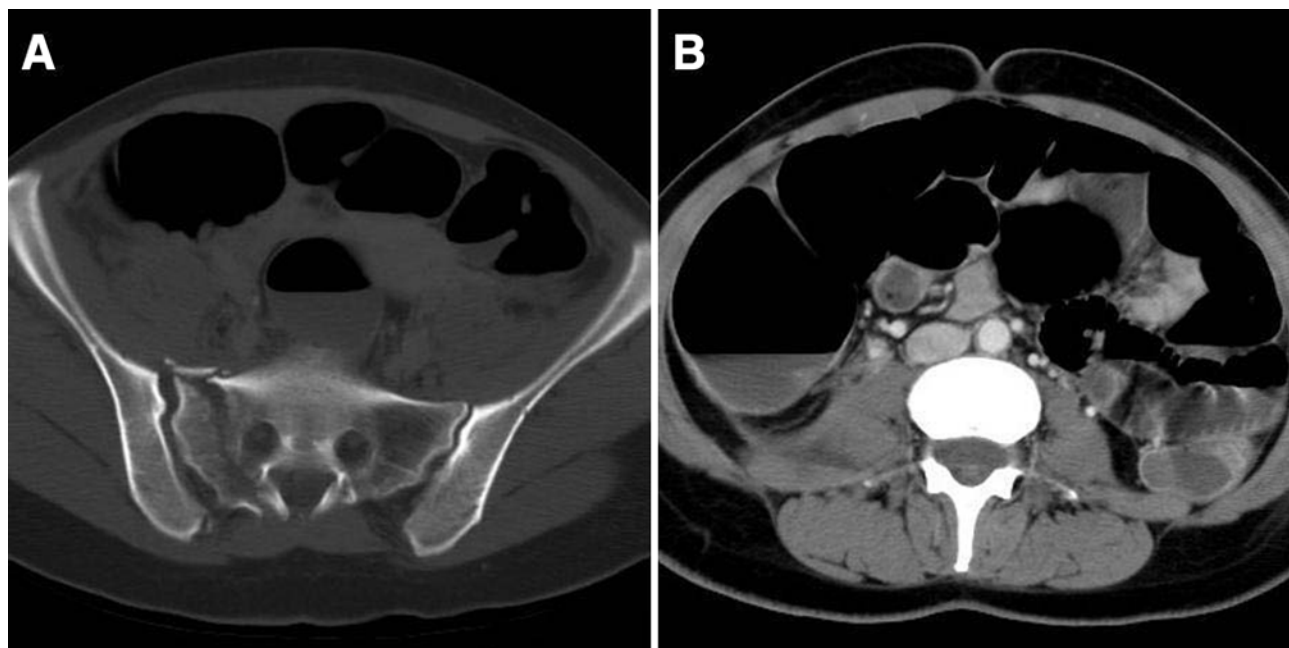


Fig. 12. Complex polytrauma with multiple pelvic fractures following voluntary defenestration in a 43-year-old female psychiatric patient. Images from total-body contrast-en-

hanced CT show right sacral wing fracture (A) and associated ipsilateral psoas muscle thickening with surrounding fluid (B)

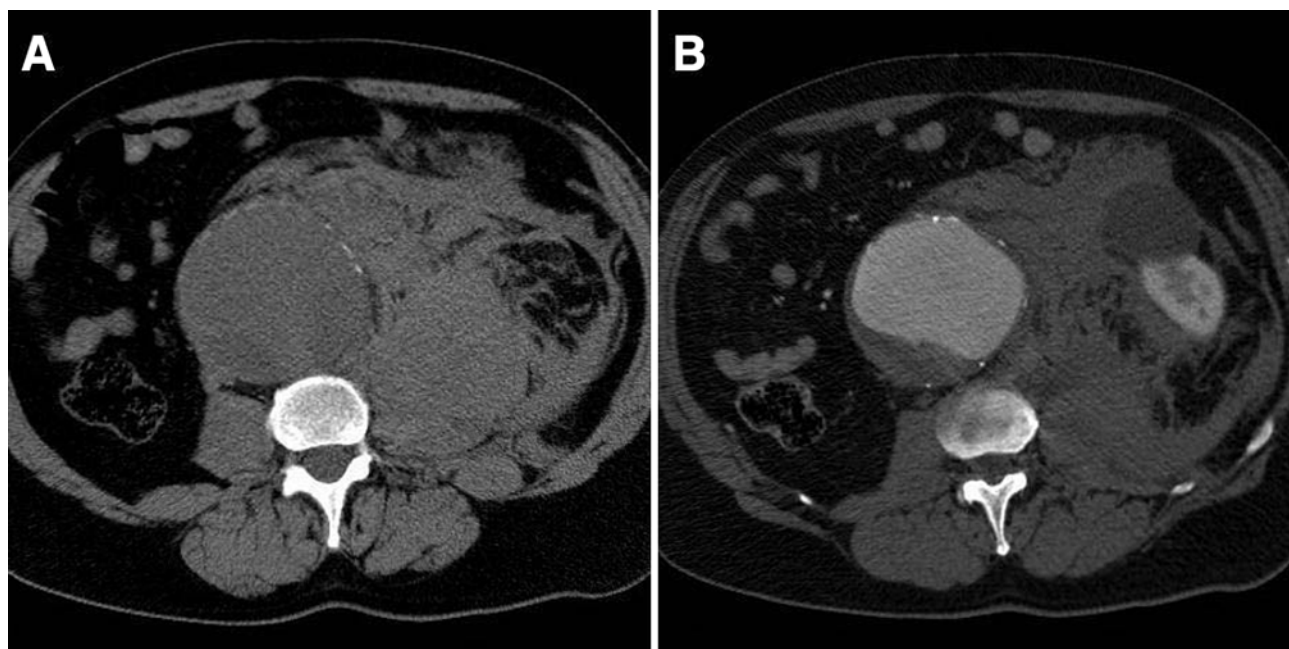
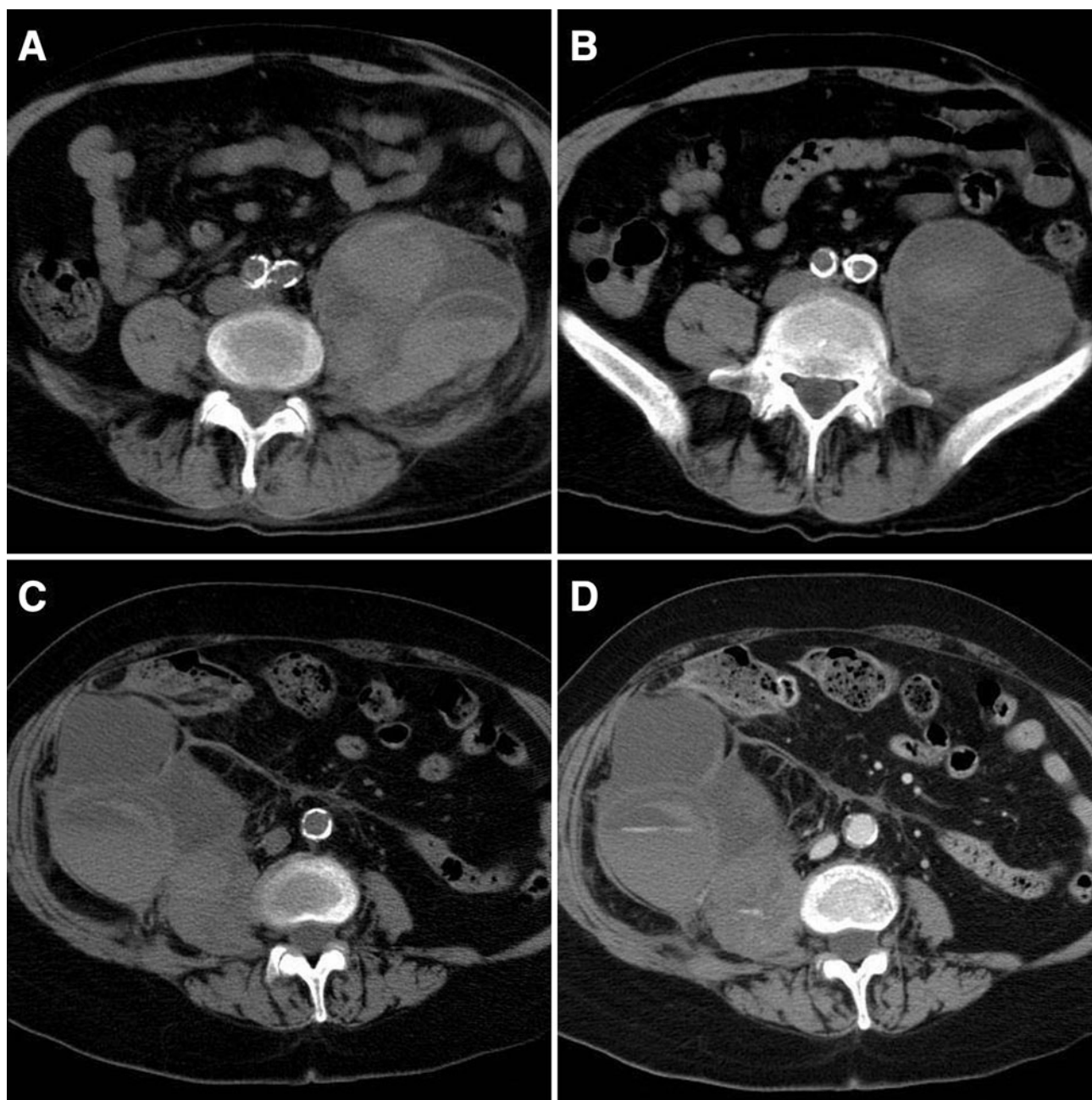


Fig. 13. Shock and intractable abdominal pain in a 64-year-old man. Emergency unenhanced (A) and CT-angiography (B) images show previously unknown, rupturing 10-cm

abdominal aortic aneurysm with abundant left retroperitoneal hemorrhage invading the psoas muscle, displacing the kidney ventrally



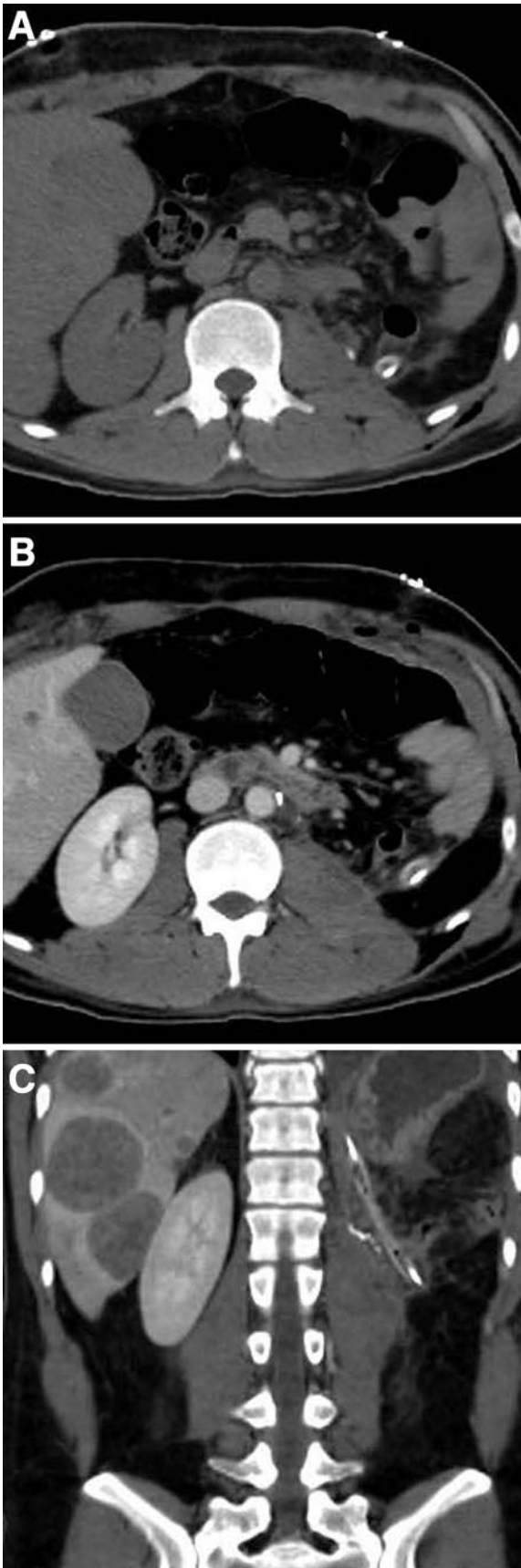
**Fig. 14.** 72-year-old man with aortic valve prosthesis receiving chronic anticoagulant therapy. Unenhanced CT acquired due to suspected renal colic (**A**) shows partly hyperdense enlargement of the left psoas muscle with fluid–fluid levels consistent with hemorrhage. Follow-up CT scan after 5 days (**B**) shows reduction of the hematoma with

decreased attenuation values. Excessive anticoagulation in 83-years-old lady. Unenhanced (**C**) and CT-angiography (**D**) images depict large right retroperitoneal and psoas hematoma with hemorrhagic levels and double active contrast extravasation; the lesion resolved after therapy discontinuation

*Trauma.* When assessing patients with penetrating or blunt body trauma, physical examination findings and laboratory tests can be unreliable in detecting organ injuries, particularly involving the retroperitoneum: therefore, CT imaging plays a key role because it allows

fast and accurate diagnosis of injuries to the retroperitoneal organs and large vessels, with simultaneous detection of spinal and pelvic fractures [28–30].

Although rare, retroperitoneal hemorrhage can represent a clinically occult yet important cause of blood



◀ Fig. 15. 29-year-old male patient who underwent resection of huge sarcoma with splenectomy, pancreatic resection and left nephrectomy. During intervention, surgeons reported to cause and suture breaches in the left hemidiaphragm and psoas fascia. One day after surgery, axial unenhanced (A), contrast-enhanced (B), and coronal-reformatted (C) image show thickening of the left psoas muscle with fascial fluid consistent with intraoperative lesion. Note adjacent surgical drainage, ipsilateral pleural effusion, and liver metastases

loss in trauma patients: CT provides confident identification of presence, site, source, and entity of retroperitoneal bleeding, and allows correct patient management particularly with sparing of unnecessary surgery [28]. Retroperitoneal hematoma involving the iliopsoas compartment (Fig. 12) is often associated with pancreatoduodenal, adrenal, and kidney injuries, with vertebral and pelvic fractures, so these abnormalities should be sought with care.

*Ruptured abdominal aortic aneurysm.* Nontraumatic “spontaneous” abdominal hemorrhage, manifested by severe pain and variable degrees of falling serum hematocrit often reaching a hypovolemic shock picture, represents a common challenge for the on-call radiologist [29].

Prompt detection of ruptured aortic aneurysm is imperative, and usually represent a straightforward diagnosis at emergency abdominal CT with the usual picture including abdominal aortic aneurysm (probability of rupture increases with diameter and is very small under 5 cm) accompanied by a retroperitoneal hematoma, sometimes involving the iliopsoas muscles (Fig. 13); active extravasation, when present, comes from the site of the aneurysmal leak [29, 31].

*Iatrogenic retroperitoneal hemorrhage due to anticoagulation.* Retroperitoneal bleeding may rarely be caused by rupture of a vascularized tumor such as a renal angiomyolipoma [2], or associated with cirrhosis or other bleeding disorders; currently, the most frequent cause is by far represented by anticoagulant therapy [29, 32]. Occurrence of iliac or psoas muscle hematoma during heparin or warfarin therapy is an infrequent yet well-recognized complication of anticoagulant therapy. Usually unilateral, this condition is variably symptomatic from lumbosacral pain and lumbar plexus symptoms, to acute abdomen with shock. Usually, coagulation assays such as activated partial thromboplastin time (APTT) and prothrombin time international normalized ratio (PT-INR) values exceed the normal limits, but sometimes this complication is observed with clotting function within normal or thera-

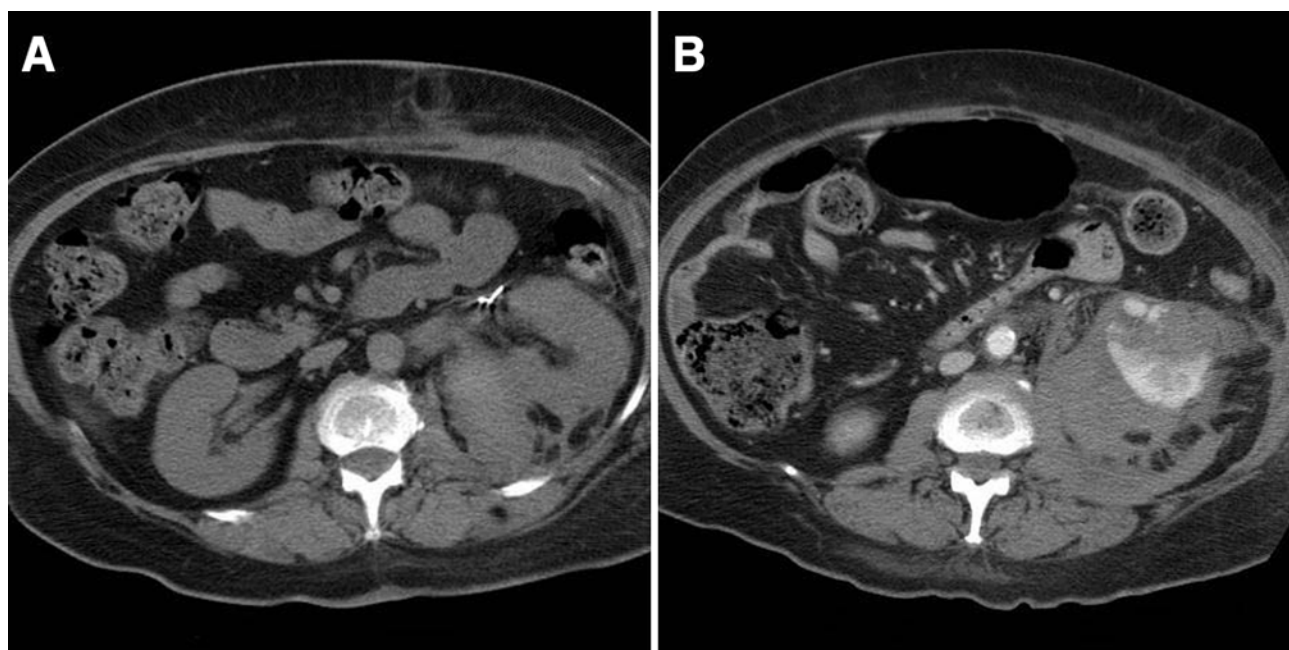


**Fig. 16.** Abdominal pain and hypotension in a 62-year old woman 8 h after laparoscopic partial nephrectomy for small renal cell carcinoma. Unenhanced (**A**) and arterial-phase contrast CT (**B**) depict hyperdense medial perirenal hemor-

rhage with active extravasation at the resected inferior renal pole, involving the ipsilateral psoas; the lesion resolved completely at 6-months follow-up

peutic range. Treatment of iatrogenic retroperitoneal hematomas is usually conservative, whereas surgery is usually risky and contraindicated though some Authors recommend decompression in cases of life-threatening occurrences [32, 33].

At CT, coagulopathic iliopsoas hemorrhage is represented by a variable-sized hematoma with the “hematocrit effect” usually present (reported in 87% of cases) as a highly sensitive and specific sign (Fig. 14) [29]. Considering the increasing possibility of concomitant diagnosis of abdominal aortic aneurysm and retroperitoneal hematoma in patients under anticoagulation medications, Federle et al. pinpointed the usefulness of the hematocrit sign (exceptionally associated with aneurismal rupture) and of active contrast extravasation (observed distant from the aorta) (Fig. 14) [29].

## Postoperative complications

Given the growing number of percutaneous instrumentation, ablation procedures, open, and laparoscopic surgical interventions, it is reasonable to expect a rise in diagnoses of different procedural complications involving the iliopsoas compartment [2]. Knowledge of interventions, normal postoperative appearance, and their potential complications is important, together with prompt cross-sectional imaging evaluation when clinical and laboratory features suggest potential complications:

multidetector CT with unenhanced, arterial and excretory phase acquisition obtained as needed, is particularly suited to provide accurate diagnosis and obtaining essential information to guide therapeutic decisions [34, 35].

## Hemorrhages

Retroperitoneal bleeding may be observed as a complication of open (Fig. 15) or laparoscopic (Fig. 16) interventions, particularly after urologic surgery. Hemorrhage is the most frequent complication of nephrectomy, usually for malignant diseases, with a nonnegligible mortality [36]. Hematoma after urologic laparoscopy has been reported to complicate 0.9%–9% of laparoscopic urologic interventions [37–39]. In the early postoperative setting, multidetector CT allows identification of presence and site of hematoma, as well as of site and entity of contrast

**Fig. 17.** 51-year-old HIV-positive woman with large non-▶ Hodgkin lymphoma of the left kidney (**A**). Postoperative CT after surgical nephrectomy show large horseshoe-shaped abscess in the left hemiabdomen (**B**), extending caudally to the iliac region (**C**), and treated with percutaneous drainage (**D**). One month later, after drainage removal, coronal (**E**) and sagittal (**F**) reformatted images from follow-up CT document small residual collection in the psoas muscle belly



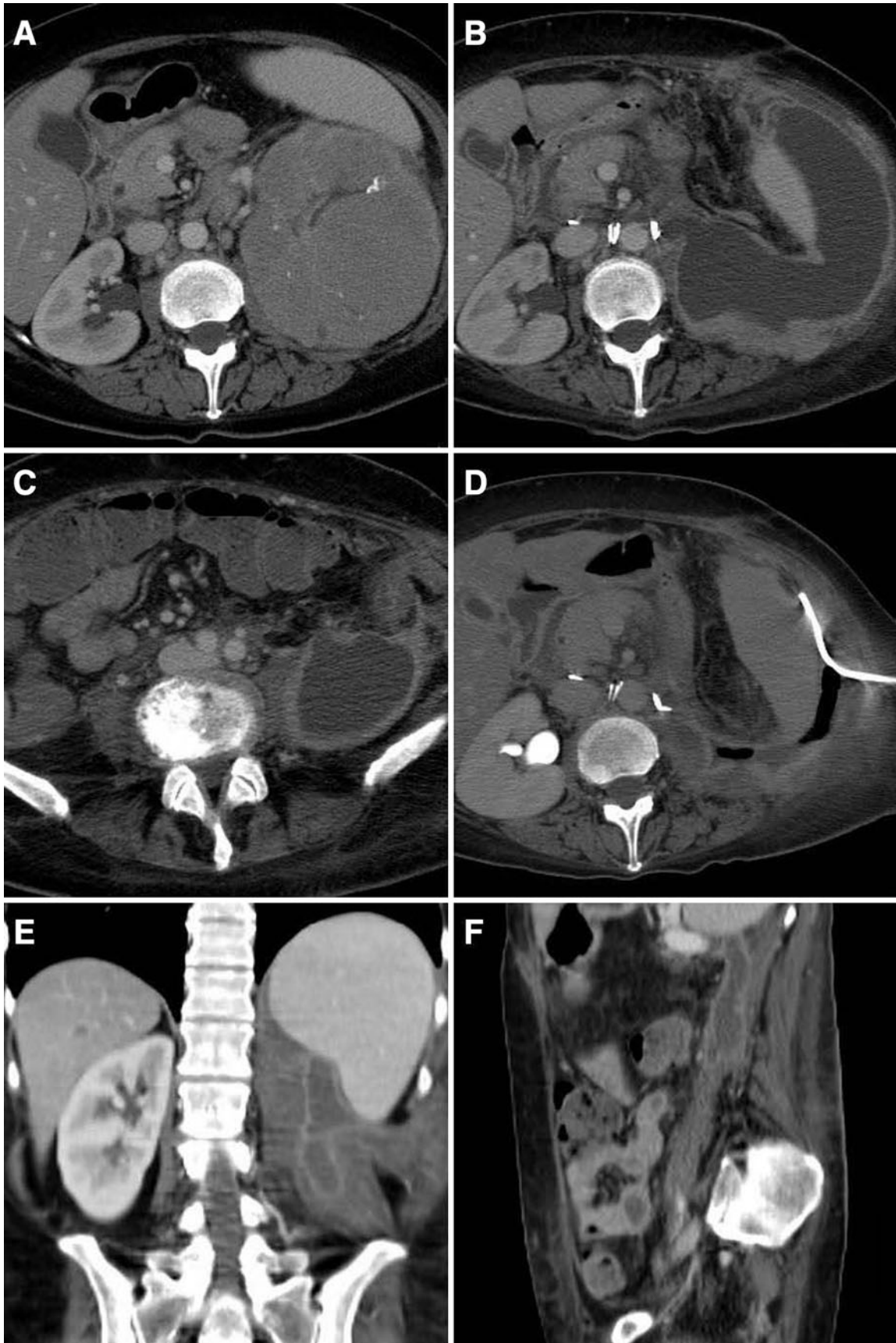




**Fig. 18.** Small iatrogenic abscess detected as an incidental finding during follow-up CT in a 73-year-old man 3 months after radical cystectomy for bladder carcinoma. Fluid collection with some air and metallic clips is seen abutting the thin left ureter, attributed to operative ureteral lesion during orthotopic bladder reconstruction

extravasation in the arterial phase indicative of active bleeding (Fig. 16), a finding that may prompt endovascular management with transcatheter embolization [40].

### *Postoperative abscess collections*

As discussed in the previous instalment, CT is the mainstay imaging modality to diagnose iliopsoas infections: their usual findings including muscle enlargement and hypodensity with indistinct margins, peripheral rim enhancement, and sometimes gas bubbles [5, 7].

Iatrogenic iliac and psoas abscesses most commonly result from urologic surgery such as nephrectomy (Fig. 17) or urinary diversion procedures (Fig. 18) [34, 35].

Alternatively, detection of an iliopsoas abscess collection may represent the paraspinal component of a postoperative discovertebral infection following orthopedic procedures performed in the groin, lumbar or hip areas, complications that are usually best visualized by MRI (Fig. 19) [15, 41, 42].

Peculiar problems in the postoperative spine may arise from the presence of metallic implants that may

determine artifacts on both CT and MRI images with significant impairment of the diagnostic quality of studies. During MRI, the acquisition protocol should avoid Gradient-Echo sequences and fat-suppression techniques, to rely mostly on conventional Turbo/Fast Spin-Echo sequences using long echo train, thinner slices, wide receiver bandwidth, and frequency-phase swap [15, 41, 42]. Beam-hardening CT artifacts may be reduced with useful diagnostic results by adopting a high milliamperage-second and 140 kVp technique coupled with submillimeter collimation, smooth reconstruction algorithms, and visualization by means of multiplanar thick-slab reformations and three-dimensional volume rendering (Fig. 19) [43, 44].

### *Urine leaks and urinomas*

Post-surgical fluid collections include hematoma, abscess, lymphocele, and urinoma in their differential diagnosis. The uncommon urinoma is defined by a confined collection of extravasated urine, resulting from iatrogenic (rarely traumatic) injury to the urinary collecting system [7, 45]. Urine leak is usually observed after urologic, retroperitoneal, gynecologic or pelvic surgery, or as a result of iatrogenic injury during instrumentation procedures such as percutaneous nephrostomy, ureteral stent placement, percutaneous nephrolithotomy, or ureteroscopic stone removal [45, 46]. Urine leak is less frequent than postoperative bleeding after open or laparoscopic surgery, with a maximal incidence reported to approach 7% [36, 38].

More commonly retroperitoneal than intraperitoneal, urinomas may sometimes involve the iliopsoas compartment (Fig. 20): at CT the key findings are fluid density (0–20 HU) and progressive enhancement in the delayed acquisitions after contrast injection because of contrast material accumulation. Excretory phase imaging (10–20 min after iodinated contrast injection) or CT-urography is, therefore, crucial for distinguishing a urinoma from other types of postoperative fluid collections (Fig. 20) [45, 47].

Sometimes, MRI may be also useful in detecting leakage from the collecting systems after urological procedures and differentiation from hemorrhage thanks to the fluid-like signal of extravasated urine (Fig. 21).

Furthermore, postoperative septic, urinary, and hemorrhagic complications may be observed in association or succession in the same patient (Fig. 10). A fluid collection such as a urinoma, hematoma, or lymphocele may become infected, resulting in an abscess: suggesting features include air bubbles in a fluid collection with a thickened and enhancing border.



**Fig. 19.** 52 year-old woman after vertebral stabilization for scoliosis correction. Volume-rendered CT image (**A**) shows metallic implants. MRI (postcontrast sagittal T1-weighted image in **B**) acquired 2 weeks after surgery to investigate persistent fever and back stiffness shows extensive posterior paravertebral collection abscess, without blood content. After

re-intervention with abscess drainage and removal of interpeduncular screws, follow-up MRI examination (postcontrast fat-suppressed sagittal T1-weighted image in **C**, axial T1 image in **D**) shows nearly complete resolution of the large abscess with a small fascial residual collection on the right, and a small psoas abscess on the left side

## Conclusions

Pathologic conditions involving the iliopsoas muscle compartment usually represent a difficult clinical diagnosis owing to the deep-seated location: the suspicion of

retroperitoneal lesions should prompt clinicians to request urgent cross-sectional imaging studies.

State-of-the art cross-sectional imaging modalities allow early detection, comprehensive visualization and confident characterization of neoplastic iliopsoas lesions,

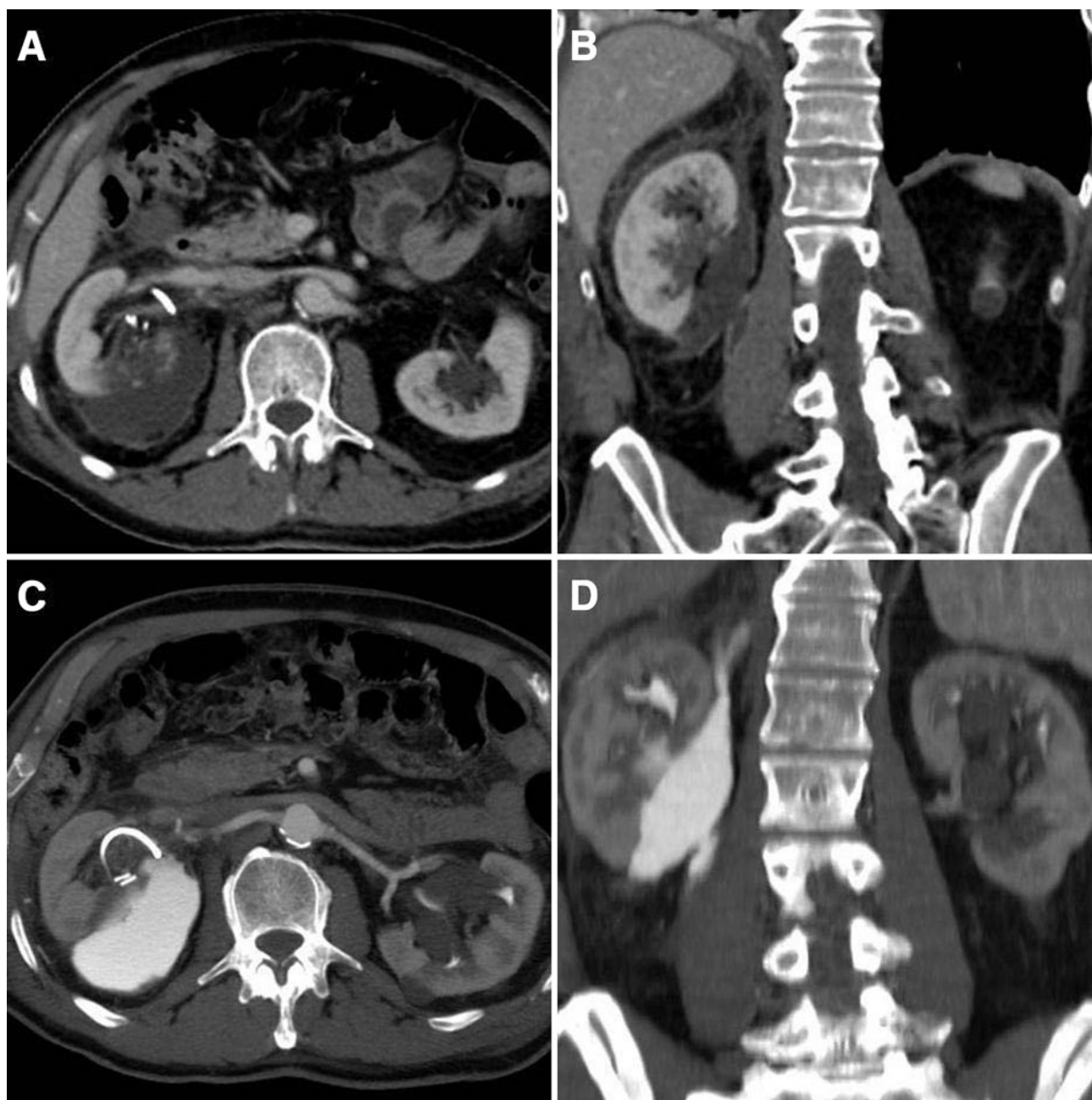


**Fig. 20.** 73-year-old man with cardiac pacemaker. After right renal tumorectomy, perirenal fluid collection is seen, along with ureteral stent and clips at the renal hilum (**A**, **B**). 48 h

later, follow-up CT with excretory phase acquisition shows the urinoma filled with enhanced urine (**C**) and communicating with the psoas through a fascial breach (**D**)

purulent and mycobacterial infections, and provide the possibility to guide percutaneous biopsy and drainage.

Knowledge of percutaneous, laparoscopic and open surgical procedures, of normal postoperative appearances and potential complications is needed to confidently diagnose, stage and follow-up most iliopsoas hemorrhagic and iatrogenic abnormalities.

Multidetector CT and MRI acquisitions allow fast and accurate diagnosis of retroperitoneal postprocedure complications, provide essential information to guide therapeutic decisions and the possibility to guide biopsy and aspiration when needed. Special attention should be paid by radiologists when choosing the optimal imaging modality and technique to allow the detection of active

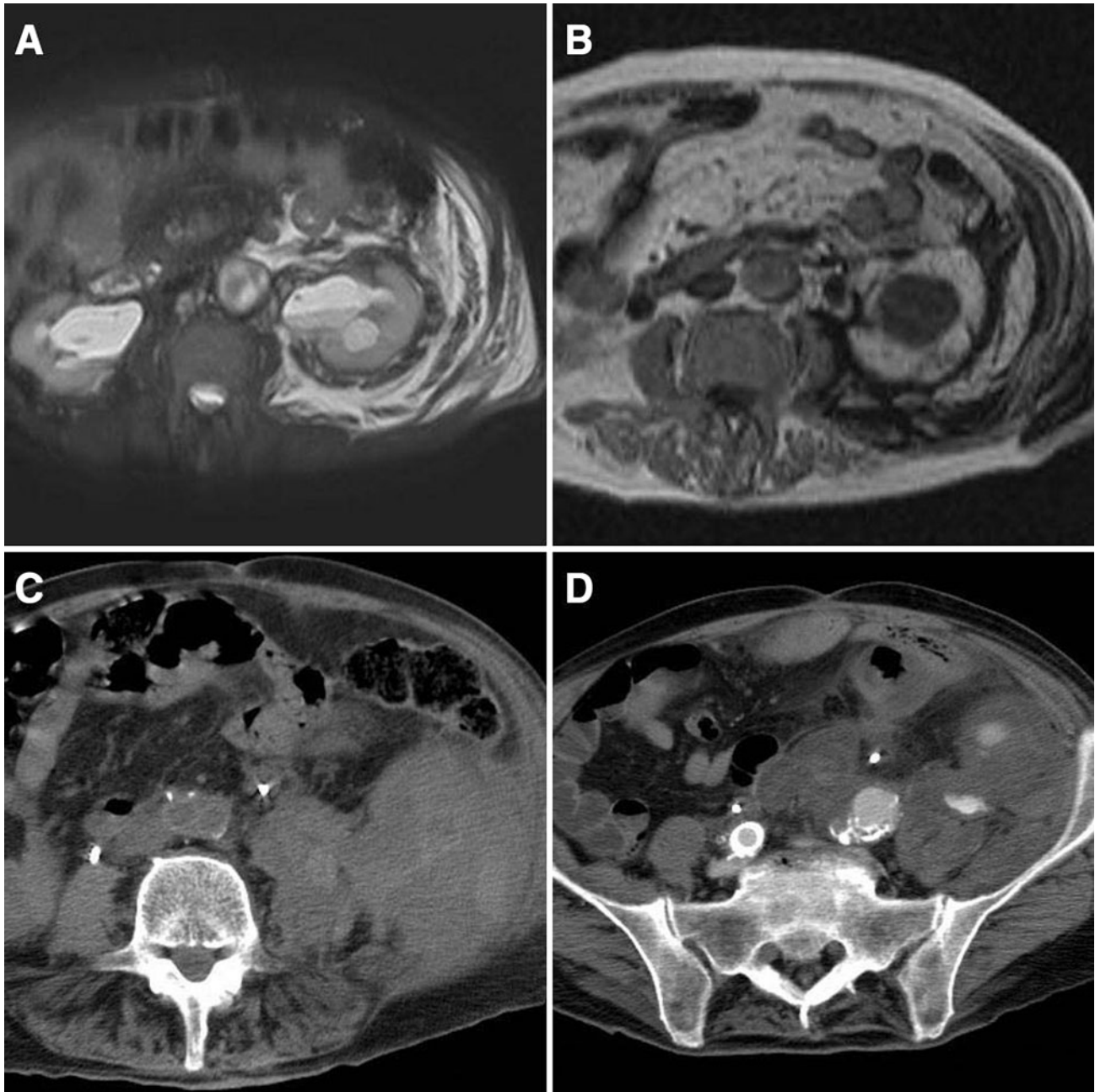


**Fig. 21.** 75-year-old male patient with retroperitoneal fibrosis. After surgical bilateral ureteral decompression, axial T2- (A) and T1-weighted (B) images show extensive peri- and pararenal fluid consistent with urine extravasation. Bilaterally dilated urinary collecting systems with level in the left renal pelvis consistent with pyonephrosis. During left ureteral stent

placement, accidental iatrogenic lesion occurred involving the ureter and the adjacent internal iliac artery, causing ipsilateral retroperitoneal hemorrhage involving the psoas muscle and characteristically hyperdense on unenhanced CT image (C), with active extravasation on arterial-phase enhanced CT acquisition (D)

hemorrhage or urinary leak, and to overcome metallic implant-related artifacts.

## References

1. Torres GM, Cernigliaro JG, Abbitt PL, et al. (1995) Iliopsoas compartment: normal anatomy and pathologic processes. *Radiographics* 15:1285–1297
2. Cronin CG, Lohan DG, Meehan CP, et al. (2008) Anatomy, pathology, imaging and intervention of the iliopsoas muscle revisited. *Emerg Radiol* 15:295–310
3. Muttarak M, Peh WC (2000) CT of unusual iliopsoas compartment lesions. *Radiographics* 20(Spec No):S53–S66
4. Mallick IH, Thoufeeq MH, Rajendran TP (2004) Iliopsoas abscesses. *Postgrad Med J* 80:459–462
5. Fayad LM, Carrino JA, Fishman EK (2007) Musculoskeletal infection: role of CT in the emergency department. *Radiographics* 27:1723–1736

6. van den Berge M, de Marie S, Kuipers T, Jansz AR, Bravenboer B (2005) Psoas abscess: report of a series and review of the literature. *Neth J Med* 63:413–416
7. Zissin R, Gayer G, Kots E, et al. (2001) Iliopsoas abscess: a report of 24 patients diagnosed by CT. *Abdom Imaging* 26:533–539
8. Charalampopoulos A, Macheras A, Charalabopoulos A, Fotiadis C, Charalabopoulos K (2009) Iliopsoas abscesses: diagnostic, aetiological and therapeutic approach in five patients with a literature review. *Scand J Gastroenterol* 44:594–599
9. Thomas A, Albert AS, Bhat S, Sunil KR (1996) Primary psoas abscess—diagnostic and therapeutic considerations. *Br J Urol* 78:358–360
10. Gayer G, Apter S, Zissin R (2002) Typhlitis as a rare cause of a psoas abscess. *Abdom Imaging* 27:600–602
11. Lobo DN, Dunn WK, Iftikhar SY, Scholefield JH (1998) Psoas abscesses complicating colonic disease: imaging and therapy. *Ann R Coll Surg Engl* 80:405–409
12. Van Dongen LM, Lubbers EJ (1982) Psoas abscess in Crohn's disease. *Br J Surg* 69:589–590
13. Veroux M, Angriman I, Ruffolo C, et al. (2004) Psoas abscess: a rare complication of Crohn's disease. *Acta Chir Belg* 104:187–190
14. Gorgulu S, Komurcu M, Silit E, Kocak I (2002) Psoas abscess as a complication of pyogenic sacroiliitis: report of a case. *Surg Today* 32:443–445
15. Longo M, Granata F, Ricciardi K, Gaeta M, Blandino A (2003) Contrast-enhanced MR imaging with fat suppression in adult-onset septic spondylodiscitis. *Eur Radiol* 13:626–637
16. Macedo TA, Stanson AW, Oderich GS, et al. (2004) Infected aortic aneurysms: imaging findings. *Radiology* 231:250–257
17. Yacoub WN, Sohn HJ, Chan S, et al. (2008) Psoas abscess rarely requires surgical intervention. *Am J Surg* 196:223–227
18. Harrigan RA, Kauffman FH, Love MB (1995) Tuberculous psoas abscess. *J Emerg Med* 13:493–498
19. Akhan O, Pringot J (2002) Imaging of abdominal tuberculosis. *Eur Radiol* 12:312–323
20. Theodorou DJ, Theodorou SJ, Kakitsubata Y, Sartoris DJ, Resnick D (2001) Imaging characteristics and epidemiologic features of atypical mycobacterial infections involving the musculoskeletal system. *AJR Am J Roentgenol* 176:341–349
21. Restrepo CS, Lemos DF, Gordillo H, et al. (2004) Imaging findings in musculoskeletal complications of AIDS. *Radiographics* 24:1029–1049
22. Bernaerts A, Vanhoenacker FM, Parizel PM, et al. (2003) Tuberculosis of the central nervous system: overview of neuroradiological findings. *Eur Radiol* 13:1876–1890
23. Gouliamos AD, Kehagias DT, Lahanis S, et al. (2001) MR imaging of tuberculous vertebral osteomyelitis: pictorial review. *Eur Radiol* 11:575–579
24. Jung NY, Jee WH, Ha KY, Park CK, Byun JY (2004) Discrimination of tuberculous spondylitis from pyogenic spondylitis on MRI. *AJR Am J Roentgenol* 182:1405–1410
25. Fitoz S, Atasoy C, Yagmurlu A, Akyar S (2001) Psoas abscess secondary to tuberculous lymphadenopathy: case report. *Abdom Imaging* 26:323–324
26. Singh AK, Gervais DA, Hahn PF, Mueller PR (2008) Neoplastic iliopsoas masses in oncology patients: CT findings. *Abdom Imaging* 33:493–497
27. Surov A, Hainz M, Holzhausen HJ, et al. (2010) Skeletal muscle metastases: primary tumours, prevalence, and radiological features. *Eur Radiol* 20:649–658
28. Daly KP, Ho CP, Persson DL, Gay SB (2008) Traumatic retroperitoneal injuries: review of multidetector CT findings. *Radiographics* 28:1571–1590
29. Federle MP, Pan KT, Pealer KM (2007) CT criteria for differentiating abdominal hemorrhage: anticoagulation or aortic aneurysm rupture? *AJR Am J Roentgenol* 188:1324–1330
30. Theumann NH, Verdon JP, Mouhsine E, et al. (2002) Traumatic injuries: imaging of pelvic fractures. *Eur Radiol* 12:1312–1330
31. Rakita D, Newatia A, Hines JJ, Siegel DN, Friedman B (2007) Spectrum of CT findings in rupture and impending rupture of abdominal aortic aneurysms. *Radiographics* 27:497–507
32. Wada Y, Yanagihara C, Nishimura Y (2005) Bilateral iliopsoas hematomas complicating anticoagulant therapy. *Intern Med* 44:641–643
33. Sasson Z, Mangat I, Peckham KA (1996) Spontaneous iliopsoas hematoma in patients with unstable coronary syndromes receiving intravenous heparin in therapeutic doses. *Can J Cardiol* 12:490–494
34. Catala V, Sola M, Samaniego J, et al. (2009) CT findings in urinary diversion after radical cystectomy: postsurgical anatomy and complications. *Radiographics* 29:461–476
35. Kawamoto S, Fishman EK (2010) Role of CT in postoperative evaluation of patients undergoing urinary diversion. *AJR Am J Roentgenol* 194:690–696
36. Beisland C, Medby PC, Sander S, Beisland HO (2000) Nephrectomy—indications, complications and postoperative mortality in 646 consecutive patients. *Eur Urol* 37:58–64
37. Parsons JK, Varkarakis I, Rha KH, et al. (2004) Complications of abdominal urologic laparoscopy: longitudinal five-year analysis. *Urology* 63:27–32
38. Simon SD, Castle EP, Ferrigni RG, et al. (2004) Complications of laparoscopic nephrectomy: the Mayo clinic experience. *J Urol* 171:1447–1450
39. Soulie M, Salomon L, Seguin P, et al. (2001) Multi-institutional study of complications in 1085 laparoscopic urologic procedures. *Urology* 58:899–903
40. Taneja M, Tan KT (2008) Renal vascular injuries following nephron-sparing surgery and their endovascular management. *Singapore Med J* 49:63–66
41. Ross JS (2000) Magnetic resonance imaging of the postoperative spine. *Semin Musculoskelet Radiol* 4:281–291
42. Yang H, Wang R, Luo T, et al. (2009) MRI manifestations and differentiated diagnosis of postoperative spinal complications. *J Huazhong Univ Sci Technol Med Sci* 29:522–526
43. Douglas-Akinwande AC, Buckwalter KA, Rydberg J, Rankin JL, Choplin RH (2006) Multichannel CT: evaluating the spine in postoperative patients with orthopedic hardware. *Radiographics* 26(Suppl 1):S97–S110
44. Ohashi K, El-Khoury GY, Bennett DL, Restrepo JM, Berbaum KS (2005) Orthopedic hardware complications diagnosed with multi-detector row CT. *Radiology* 237:570–577
45. Titton RL, Gervais DA, Hahn PF, et al. (2003) Urine leaks and urinomas: diagnosis and imaging-guided intervention. *Radiographics* 23:1133–1147
46. Carrafello G, Lagana D, Mangini M, et al. (2006) Complications of percutaneous nephrostomy in the treatment of malignant ureteral obstructions: single-centre review. *Radiol Med* 111:562–571
47. Van Der Molen AJ, Cowan NC, Mueller-Lisse UG, et al. (2008) CT urography: definition, indications and techniques. A guideline for clinical practice. *Eur Radiol* 18:4–17